Brain Topography (2020) 33:450–460
https://doi.org/10.1007/s10548-020-00780-7

ORIGINAL PAPER

EEG Electric Field Topography is Stable During Moments of High Field Strength

Anthony P. Zanesco[1]

Received: 5 June 2019 / Accepted: 2 June 2020 / Published online: 8 June 2020

Abstract

Spontaneous broadband electroencephalography (EEG) demonstrates short moments of stability in the spatial distribution of the head-surface voltage topography. This phenomenon underlies the premise behind segmenting multichannel EEG into topographically defined brain states, known as EEG *microstates*. Microstate segmentation methods commonly identify representative topographical configurations based on clustering applied to a subset of voltage maps selected at the time series points of greatest strength in the neuroelectric field. These moments are well-reasoned to best represent periods of momentary stability in the voltage topography, and consequently, points of greatest signal relative to noise. Yet, more direct empirical evidence for these assumptions is warranted, and the consistency of this phenomenon across individuals has not been characterized. In the present investigation, the association between electric field strength and topographic dissimilarity of temporally adjacent samples of EEG were characterized in a large sample of healthy adults engaged in quiet rest. Samples of individuals' EEG time series high in electric field strength were found to be topographically similar relative to adjacent time series samples. The strong phase-synchronized actvity of neuronal populations therefore coincides with momentary stability in the topographic voltage configuration, providing robust empirical support for the basic premise underlying segmentation of broadband EEG into microstates.

Keywords EEG · Global field power · Microstates · Topographic dissimilarity

Scalp recorded broadband electroencephalography (EEG) exhibits moments of spontaneous topographic stability that appear to be fundamental to the coordinated dynamics of the neuroelectric field. When carefully examined over short time scales, the spatial distribution of the head-surface voltage topography plotted as a succession of three-dimensional voltage maps gives the impression of short periods of stability, in which a particular topographic configuration predominates momentarily (~40–120 ms) before quickly transitioning to a different quasi-stable configuration. Moreover, the same topographic configurations appear to be common to a large portion of the voltage maps present during these periods of quasi-stability. These observations underlie the premise behind the segmentation of multichannel EEG time series into *microstates* based on clustering of topographic patterns to identify the millisecond spatiotemporal dynamics of coordinated brain states (Lehmann et al. 1987; Wackermann et al. 1993).

Spatial decomposition of EEG time series into microstates has consistently identified a limited set of data-driven clusters of voltage maps that explain a large portion of observed topographic variance (see for review, Khanna et al. 2015; Michel and Koenig 2018). Each distinct topographic configuration of voltage distribution implies by physical laws different distributions of active neural generators in the brain (Vaughan 1982), allowing topography

I thank the Mind-Body-Emotion group at the Max Planck Institute for Human Cognitive and Brain Sciences who gathered and made available the de-identified data on which this manuscript is based. I utilized the freely available Cartool software toolbox (cartoolcommunity.unige.ch) programmed by Denis Brunet, from the Functional Brain Mapping Laboratory, Geneva, Switzerland, and supported by the Center for Biomedical Imaging of Geneva and Lausanne. The data supporting the findings of this study are openly available in the OSF repository and can be found at: https://osf.io/7bcem/.

Handling Editor: Christoph M. Michel.

✉ Anthony P. Zanesco
apz13@miami.edu

[1] Department of Psychology, University of Miami, 5665 Ponce de Leon Blvd, Coral Gables, FL 33146, USA

to be used to define changes in the activity of predominating whole-brain neuronal networks. That dozens of studies have consistently identified similar clusters of maps when segmenting spontaneous EEG into microstates, suggests a common brain network architecture underlying sources of spontaneous phase-synchronized activity observed at rest (Michel and Koenig 2018). Furthermore, the electrical brain sources of microstates align with several fMRI-derived resting state functional networks (Britz et al. 2010; Custo et al. 2017; Brechet et al. 2019). This makes the microstate approach timely given increasing interest in segmenting the spontaneous organization of brain activity into coordinated networks.

Methods of defining microstates based on topography have commonly utilized topographic clustering methods applied to a subset of voltage maps (e.g., Michel et al. 2009), selected at the local maxima in the time series of global electric field strength. These points can be quantified based on the global field power (GFP), which reflects a reference-independent measure of the strength of synchronized brain response at a moment in time (Skrandies 1990). Selecting voltage maps at local GFP maxima for topographic clustering has remained a defensible approach because of the observation that moments of strong phase-synchronized activity generally demonstrate quasi-stability in their voltage topography (Skrandies 1990). These moments are therefore suggested to reflect points of greatest signal relative to noise (Koenig and Brandeis 2016), making local peaks in the GFP time series ideal candidates for identifying quasi-stable topographic configurations present in the EEG.

The most striking evidence for these suppositions, however, come from the broad success of topographic clustering approaches in identifying common microstate configurations across studies, and the utility of segmentation procedures in defining time series sequences of microstates (Michel and Koenig 2018). Large proportions of topographic variance in the continuous EEG are therefore explained by only a few microstate cluster centroids identified from clustering of voltage maps at local peaks in the GFP time series (e.g., Seitzman et al. 2017; Zanesco et al. 2020). The centroids of clusters (i.e., microstate configurations) are subsequently used to categorize the EEG in a winner-take-all fashion according to the cluster centroid with the strongest spatial correlation between it and each voltage map in the time series. Yet, recent studies have also called into question some of the basic assumptions of the microstate approach. Namely, Mishra et al. (2020) have questioned the assumption that each voltage map in the EEG time series is best represented by only a single discrete microstate (i.e., the winner-take-all principle). This "discreteness assumption" implies that EEG data is distributed closely around a limited number of microstate configurations, and is supported by the observation that voltage maps remain in a single, relatively similar configuration for brief periods of time before quickly transitioning to other configurations.

Instead, Mishra et al. (2020) found that assumptions about topographic discreteness are most valid for peaks in the GFP time series (i.e., local GFP maxima) but are less valid when GFP is low. This makes sense in that microstate cluster configurations are themselves commonly derived from voltage maps at local GFP maxima, which are well-reasoned to reflect points of greatest signal relative to noise. But local GFP maxima can also have low GFP relative to other samples in the overall distribution. Accordingly, voltage maps with lower GFP—even those at local GFP maxima—are less likely to be best represented by only a single discrete microstate configuration (Mishra et al. 2020). This is consistent with other work demonstrating uncertainty in the microstate solution for samples with low GFP (Dinov and Leech 2017). Thus, categorizing voltage maps into classes of microstates is more probabilistic than certain, and the winner-take-all approach will lead to uncertain categorizations for some samples of the EEG time series (Dinov and Leech 2017; Mishra et al. 2020).

More empirical studies investigating the basic assumptions of the microstate approach are therefore warranted. Empirical evidence supporting the basic association between GFP and topographic stability in spontaneous EEG collected at rest has not been comprehensively reported in the literature. Koenig and Brandeis (2016), however, provided one compelling demonstration of the strong within-person association between GFP and momentary topographic stability in the EEG time series. By calculating the similarity between temporally adjacent voltage maps, they quantified fluctuations in the topographic stability of voltage maps. They then demonstrated a strong association between samples with high GFP and topographic similarity with adjacent samples in an hour-long EEG recording acquired from a single individual (Koenig and Brandeis 2016). This was an important observation, but the consistency of this phenomenon across a wider range of individuals has not been characterized.

In the present investigation, I revisit the basic premise behind EEG microstate analysis that periods of strong phase-synchronized neural activity demonstrate topographic stability for brief moments of time. In line with the approach used by Koenig and Brandeis (2016) to demonstrate this principle, I examined the consistency and variability of associations between GFP and topographic dissimilarity of adjacent samples of EEG in a large sample of healthy adults. True to the notion that strong activity of phase-synchronized neuronal populations coincides with periods of topographic stability, samples of the EEG time series high in GFP ought to be topographically similar relative to adjacent samples.

16-minutes of scalp recorded multichannel EEG were acquired from 216 healthy adults at rest by Babayan et al. (2019) and de-identified data was made publicly available

on a data-sharing repository. Resting EEG were divided into eyes closed (8-min) and eyes open (8-min) epochs. Using these data, I calculated within-person correlations between the GFP and topographic dissimilarity of temporally adjacent (*sample t* and *sample t* − 1) voltage maps for all samples of individuals' EEG recordings (Skrandies 1990; Murray et al. 2008). In addition to supporting the notion that maps at local maxima of GFP are strong indicators of momentary stability in topographic configuration, voltage maps with high field strength and stable topography ought to reflect optimal points for clustering voltage maps to obtain common patterns of global microstate configurations across individuals. To address this question, I examined the degree to which the GFP and topographic dissimilarity of voltage maps were predictive of their spatial correlation with microstate configurations identified through topographic clustering.

Methods

Participants

227 participants were recruited to participate as part of the MPI-Leipzig Mind-Brain-Body study (MPILMBB; Babayan et al. 2019). Participants were recruited as part of two separate age cohorts. The younger age cohort was between 20 and 35 years old ($N = 153$, 45 females, age $M = 25.1$ years, $SD = 3.1$) and the older age cohort was between 59 and 77 years old ($N = 74$, 37 females, age $M = 67.6$ years, $SD = 4.7$). Participants underwent an extensive medical and psychological screening procedure before inclusion (see Babayan et al. 2019). Resting EEG was recorded from 216 of these participants at the Day Clinic for Cognitive Neurology of the University Clinic Leipzig and the Max Planck Institute for Human Cognitive and Brain Sciences (MPI CBS) in Leipzig, Germany. Written informed consent was obtained prior to participating in the study, and all participants received monetary compensation. The study was carried out in accordance with the Declaration of Helsinki and the study protocol was approved by the ethics committee of the University of Leipzig (Reference #154/13-ff).

Procedure

16 min of resting EEG was acquired from 216 participants in a sound attenuated chamber prior to the administration of psychological questionnaires and assessments including a psychiatric interview (SCID; Wittchen et al. 1997). Each EEG recording was divided into 16 contiguous 1-min blocks, with two conditions interleaved, eyes closed and eyes open, beginning with the eyes closed condition. Presentation software (Neurobehavioral Systems Inc., USA) was used to indicate changes between blocks. Participants were instructed to fixate on a black cross presented on a white background during the eyes open blocks.

EEG Data Collection and Processing

Resting EEG was recorded from a 62-channel active electrode cap (ActiCAP, Brain Products GmbH, Germany), with 61 channels in the international 10–20 system arrangement and one additional electrode below the right eye recording vertical eye movements. The reference electrode was located at electrode position FCz and the ground was located at the sternum. Electrode impedance were kept below 5 kΩ. Data were acquired with a BrainAmp MR plus amplifier (Brain Products GmbH, Germany) at an amplitude resolution of 0.1 μV and sampling rate of 2500 Hz. EEG were bandpass filtered online between 0.015 Hz and 1 kHz, subsequently downsampled offline to 250 Hz, and bandpass filtered between 1 and 45 Hz (Butterworth filter, filter order 4). 8-min eyes closed and eyes open epochs were separately concatenated.

Preprocessed EEG recordings (Babayan et al. 2019) were made available for use to interested researchers on a data-sharing repository (https://ftp.gwdg.de/pub/misc/MPI-Leipzig_Mind-Brain-Body-LEMON/). As reported by Babayan et al. (2019), outlier channels with poor signal quality, extreme peak-to-peak deflections, or large bursts of high frequency activity, were excluded based on visual inspection. Principal component analysis (PCA) was used to reduce the dimensionality of the data by keeping components that explain 95% of the total data variance. Infomax independent component analysis (ICA) was used to remove components reflecting eye movements, eye blinks, or heartbeat related signal contaminants. Remaining independent components ($M = 21.4$ components, range: 14–28) were then reconstructed and projected back to sensor space. 13 participants were excluded due to missing event information, different sampling rate, or insufficient data quality.

Following collection of the 406 preprocessed EEG recordings from 203 participants from the data-sharing repository, missing electrodes were interpolated based on spherical spline interpolation to a 64-channel montage and average-referenced using the Cartool software toolbox version 3.7 (Brunet et al. 2011). To focus my analyses on healthy individuals, I excluded 12 additional participants from further analysis because the psychiatric interview conducted at the second assessment identified potential psychological concerns (e.g., substance abuse or unspecified hallucinations). This left 191 participants in the current analysis, with an average of 7.83 min ($SD = 0.51$) of eyes closed and 7.77 min ($SD = 0.53$) of eyes open resting EEG.

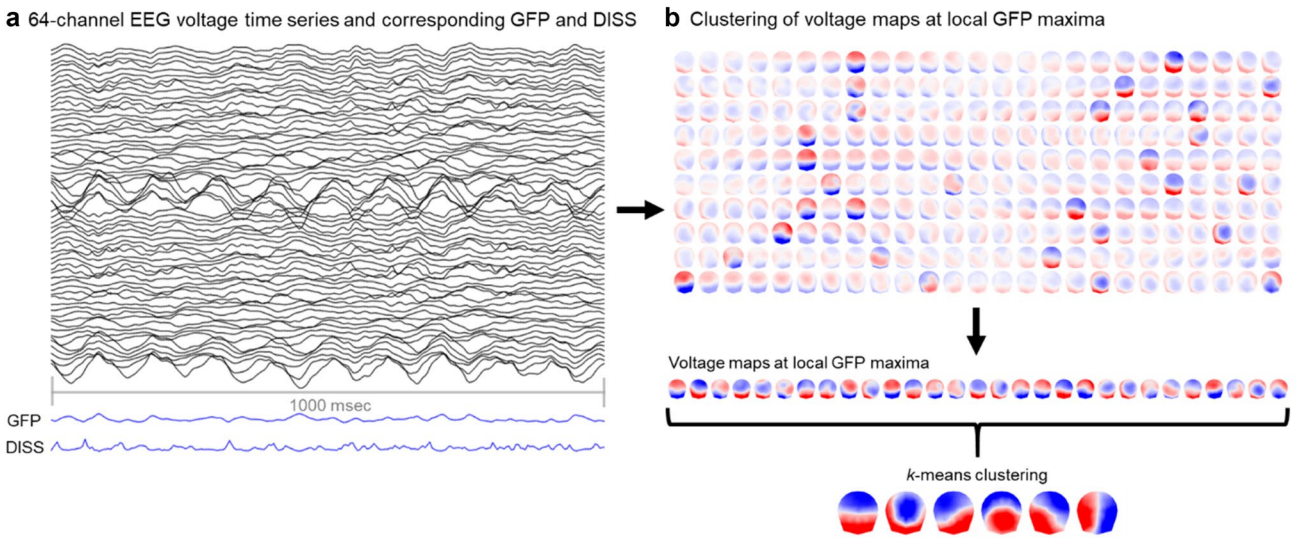

Fig. 1 One second of 64-channel eyes-closed resting EEG (sampled at 250 Hz) is shown (**a**) from a recording chosen at random. The global field power (GFP) is calculated from the multichannel EEG and reflects a measure of the ongoing strength of the electric field. The periodicity of peaks in GFP coincide with oscillations at the dominant EEG frequency. Topographic dissimilarity (DISS) is also calculated and reflects a measure of the difference in spatial configuration between electric fields of temporally adjacent (*sample t* and *sample t* – 1) voltage maps, independent of their strength. GFP appears inversely correlated with topographic dissimilarity. **b** Rows depict the time series succession of voltage maps from left to right of 1 s of EEG. Voltage maps are 2D isometric projections with nasion upwards. Voltage maps are highlighted at the local maxima in the global field power (GFP). The topography generally appears quasi-stable for several samples surrounding local GFP maxima. *k*-means clustering of maps at local GFP maxima identified six optimal subject-level topographic clusters of maps for this individual

Global Field Power and Topographic Dissimilarity

Global field power (GFP) and topographic dissimilarity (DISS) of temporally adjacent samples (*sample t* − 1) were calculated for samples of the EEG time series. GFP is a reference-independent measure of voltage potential (μV) that quantifies the strength of the scalp electric field at a given sample of the recording and is equivalent to the standard deviation of amplitude across the average-referenced electrode montage (Skrandies 1990; Murray et al. 2008). GFP was calculated for all samples of the EEG time series for the remaining 191 participants (382 total eyes closed and eyes open recordings). Furthermore, the difference in topography between temporally adjacent voltage maps was calculated based on the measure of global topographic dissimilarity (Skrandies 1990; Murray et al. 2008). DISS is quantified as the square root of the mean of squared differences between GFP normalized electrodes and reflects a measure of the overall difference in spatial configuration between two electric fields, independent of their strength. DISS was calculated between the voltage map of each time series sample (*sample t*) and the map of the preceding sample (*sample t* − 1). This quantified the topographic dissimilarity between voltage maps in subsequent moments.

Figure 1a depicts the calculation of GFP and DISS from 1 s of EEG from a participant chosen at random. High DISS indicates that the voltage map of the current sample and the preceding sample were dissimilar in spatial configuration. Values of GFP and DISS were log-transformed and the correlation between the strength of the electric field and dissimilarity of temporally adjacent voltage maps was calculated for the EEG time series of each individual recording. Correlations were compared between eyes closed and eyes open conditions with a paired *t* test after Fisher *r* to *z* transformation. In addition, the GFP and DISS of samples selected at the local GFP maxima of the EEG time series were compared to all the remaining samples of each individual recording, and the proportion of variance accounted for by local GFP maxima was examined. Figure 1b depicts the time series of voltage maps from 1 s of EEG with maps at local GFP maxima indicated. There were 14624.6 ($SD = 2371.0$) and 16669.1 ($SD = 2357.7$) samples at the local GFP maxima on average for individuals in the eyes closed and eyes open conditions, respectively. This was out of 117839.9 ($SD = 7616.2$) total EEG samples in the eyes closed condition and 116538.4 ($SD = 7918.0$) samples in the eyes open condition on average. Finally, differences in the association between GFP and DISS were examined for samples at the local GFP maxima compared to other samples. The amount of variance explained in DISS by the interaction between GFP and whether a sample was selected at the local GFP maxima was examined, over and above both main effects alone.

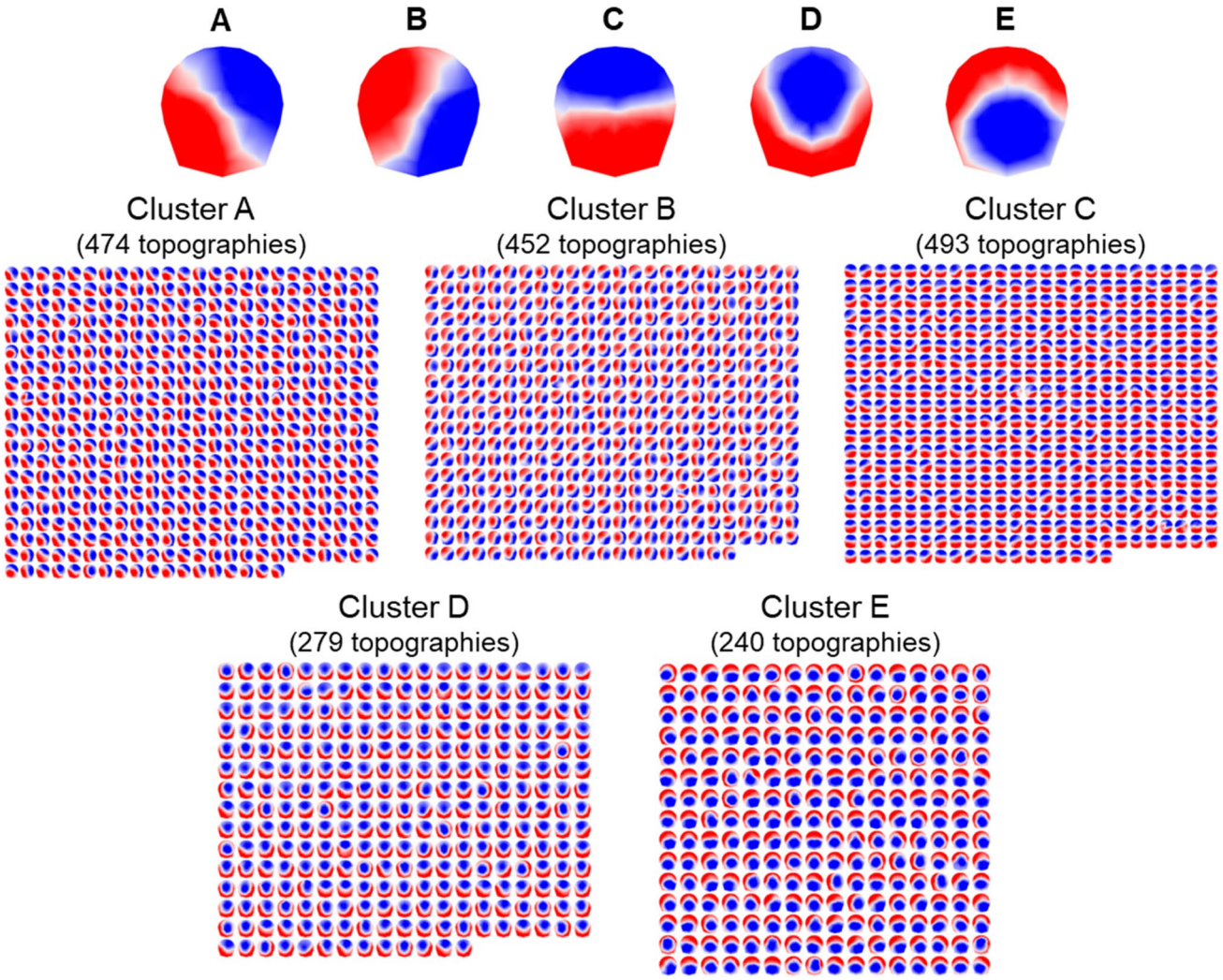

Fig. 2 Five global cluster centroids were identified from *k*-means clustering during 8-min of eyes closed and 8-min of eyes open rest. 1938 cluster centroids derived from *k*-means clustering of voltage maps at GFP peaks from 382 individual subject recordings are shown grouped according to their global cluster membership. Voltage topographies are 2D isometric projections with nasion upwards. Each global topography (A through E) is the centroid of respective clusters of maps

Topographic Clustering and Microstate Segmentation

Topographic microstate segmentation of EEG and parameterization of the microstate time series in the 191 participants (382 recordings) was previously reported in Zanesco et al. (2020). The results of topographic clustering are summarized below. Briefly, topographic clustering of voltage maps at local GFP maxima was conducted separately for each individual recording. The adapted *k*-means clustering procedure, implemented in Cartool (Brunet et al. 2011), revealed an optimal number of 4 to 8 subject-level centroid topographies (totaling 1940 topographies) for each individual EEG recording ($M = 5.08$, $SD = 0.94$) that explained 81.71% ($SD = 4.36$, range = 72.31–91.90) of GEV of centroids on average in the eyes closed condition and 78.84% ($SD = 3.45$, range = 68.76–88.37) in the eyes open condition. A second round of clustering of individual subject-level centroids revealed five global clusters that together explained 85.03% of the GEV in the 1940 individual subject-level cluster centroid topographies. These five clusters, designated as microstate configurations A through E, were retained as the optimal number of global clusters. Figure 2 depicts the five optimal global cluster centroids and the 1938 individual subject-level cluster topographies (two topographies went unassigned) grouped according to their cluster membership.

The dependence of the microstate fitting procedure on the strength and topographic stability of the electric field was also examined. Spatial correlations were calculated between GFP normalized EEG samples and each of the five global

microstate cluster centroids. Polarity was ignored when calculating spatial correlations and only the relative spatial configuration was considered. EEG were spatially smoothed in Cartool using the spatial interseptile weighted mean to minimize the influence of outliers in the electrode montage. The maximal spatial correlation between microstate cluster centroids was retained for each sample. This is in line with the winner-take-all principle commonly used to categorize samples of EEG according to the microstate that best represents each voltage map in the time series. The correlation between log-transformed GFP and DISS, and the Fisher *r* to *z*-transformed spatial correlation with microstate cluster centroids, were calculated for samples of each individual recording.

Results

Global Field Power and Topographic Temporal Stability

Within-person correlations were calculated between the GFP of each sample and the topographic dissimilarity (DISS) between temporally adjacent (*sample t* and *sample t* – 1) voltage maps for the EEG time series of each recording. Values of GFP and DISS were also log-transformed. Figure 3 depicts scatterplots demonstrating the association between GFP and DISS, and log-transformed GFP and DISS, for 4 eyes-closed and 4 eyes-open EEG recordings chosen at random. As can be seen, the DISS of temporally adjacent maps was low at points of high GFP. The reverse, however, does not appear to be true. At points of low GFP, DISS ranged across the entire distribution of values.

Strong negative correlations between log-transformed GFP and DISS were observed on average in both the eyes closed (*mean* $r = -0.658$, $SD = 0.060$, 95% CI [– 0.667, – 0.650]) and eyes open conditions (*mean* $r = -0.663$, $SD = 0.065$, 95% CI [– 0.672, – 0.654]).[1] One individual was a clear outlier overall (eyes closed $r = -0.261$ and eyes open $r = -0.311$), and there were two other outlier eyes open recordings with $r = -0.293$ and $r = -0.332$, respectively. All the remaining correlations were strongly negative and ranged from $r = -0.453$ to -0.766 for the eyes closed condition, and $r = -0.426$ to -0.766 for the eyes open condition. Figure 4 depicts the mean correlations for each condition and range of correlations among individuals.

[1] The mean correlations were nearly identical when including the 12 individuals originally excluded from the sample. Correlations for all 203 individuals were large on average in both the eyes closed (*mean* $r = -0.657$, $SD = 0.060$, 95% CI [– 0.666, – 0.649]) and eyes open conditions (*mean* $r = -0.663$, $SD = 0.064$, 95% CI [– 0.672, – 0.654]).

Fisher *z*-transformed correlations did not significantly differ between conditions, $t(190) = 1.338$, $p = 0.182$, but were positively correlated within-persons across conditions ($r = 0.582$, $p < 0.001$, 95% CI [0.480, 0.669]). These findings confirm the robust association between GFP and topographic temporal stability in a large sample of healthy adults. Voltage topography at moments of high electric field strength is therefore more temporally stable than when field strength is lower.

Global Field Power and Topographic Temporal Stability at Local GFP Maxima

The topographic dissimilarity (DISS) between temporally adjacent (*sample t* and *sample t* – 1) voltage maps was next compared between samples selected at the local GFP maxima of the EEG time series and all remaining samples. Figure 5 depicts scatterplots between GFP and DISS, and log-transformed GFP and DISS, for samples (in yellow) selected at the local GFP maxima in the EEG time series. As depicted, samples selected at the local GFP maxima have consistently lower DISS compared to the overall distribution. In contrast, local GFP maxima vary in magnitude across the entire range of the GFP distribution.

Accordingly, the log-transformed DISS of samples at the local GFP maxima was lower on average compared to all the remaining samples in both the eyes closed ($M_{diff} = -0.375$, $SD = 0.076$, 95% CI [– 0.386, – 0.364]) and eyes open conditions ($M_{diff} = -0.316$, $SD = 0.059$, 95% CI [– 0.324, – 0.308]). Whether a sample was selected at the local GFP maxima (or not) explained roughly 5% of the variance in log-transformed DISS on average in both the eyes closed (*mean* $R^2 = 0.054$, $SD = 0.012$, 95% CI [0.052, 0.056]) and eyes open conditions (*mean* $R^2 = 0.052$, $SD = 0.014$, 95% CI [0.050, 0.054]). These findings provide further support for the premise that points of local GFP maxima demonstrate greater topographic stability compared to the overall distribution of EEG samples (see Fig. 5). The basic premise of microstate segmentation that voltage maps at local GFP maxima are strong indicators of momentary stability in topographic configuration is therefore well supported by empirical data.

The log-transformed GFP of samples at the local GFP maxima was also greater on average compared to other samples in the eyes closed ($M_{diff} = 0.217$, $SD = 0.031$, 95% CI [0.213, 0.222]) and eyes open conditions ($M_{diff} = 0.205$, $SD = 0.023$, 95% CI [0.202, 0.209]). Yet, whether samples were selected at the local GFP maxima or not explained only 3% of variance in log-transformed GFP on average in the eyes closed (*mean* $R^2 = 0.031$, $SD = 0.017$, 95% CI [0.028, 0.033]) and eyes open conditions (*mean* $R^2 = 0.037$, $SD = 0.019$, 95% CI [0.034, 0.040]). It is thus unsurprising that samples selected at the local GFP

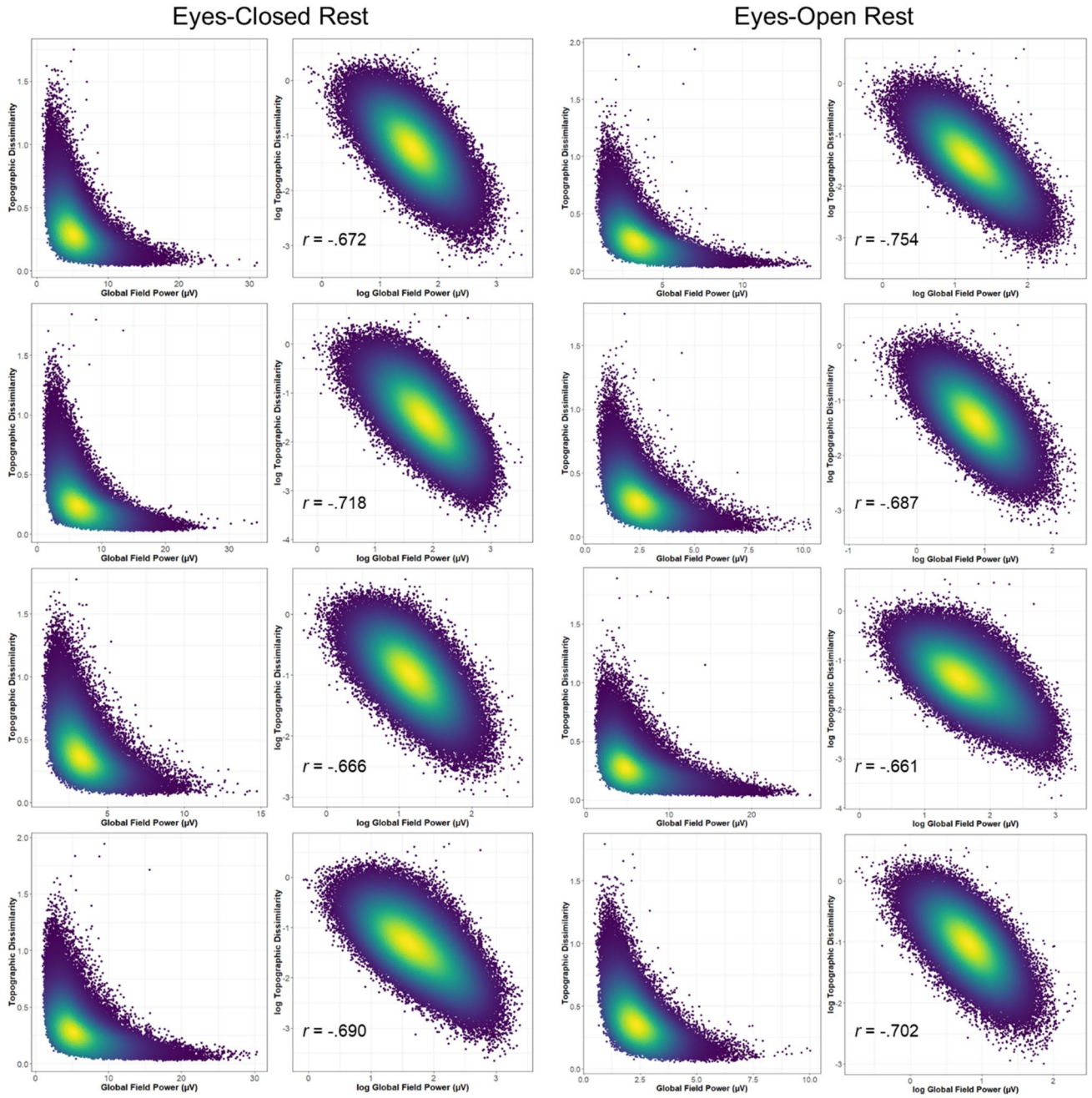

Fig. 3 Scatterplots depicting samples of global field power (GFP) by topographic dissimilarity between temporally adjacent (*sample t* and *sample t* – 1) voltage maps for four eyes closed and four eyes open EEG recordings selected at random. The left column of each pair depicts raw values and the right column depicts the corresponding log-transformed values and within-person correlation. The density of the distribution of values is indicated (from low density in purple to high density in yellow)

maxima had greater GFP amplitude than the rest of the distribution. However, it is perhaps counterintuitive that these points better differentiated the topographic dissimilarity of temporally adjacent samples than they did overall GFP amplitude (see Fig. 5).

Importantly, associations between log-transformed GFP and DISS did not differ for samples selected at the local GFP maxima compared to all remaining samples. That is, differences in how well log-transformed GFP predicted DISS between those samples selected at the local GFP maxima and all remaining

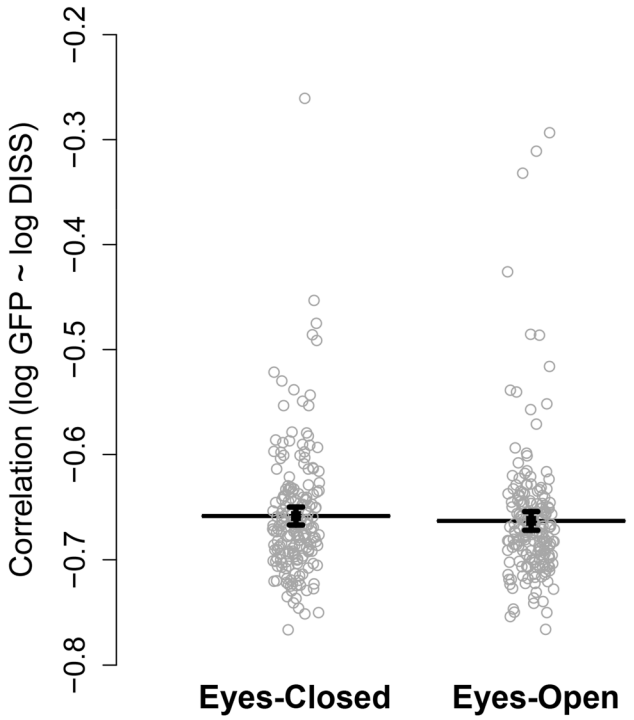

Fig. 4 Means are plotted for within-person correlations between log-transformed global field power (GFP) and topographic dissimilarity for eyes-closed and eyes-open conditions. Observed participant ($n = 191$) correlations are plotted as dots. Errors bars are 95% CI of the mean

samples explained only a negligible amount of additional variance in log-transformed DISS on average across individuals in both the eyes closed (*mean* $\Delta R^2 = 0.0007$, $SD = 0.0006$, 95% CI [0.0006, 0.0008]) and eyes open conditions (*mean* $\Delta R^2 = 0.0004$, $SD = 0.0004$, 95% CI [0.0003, 0.0005]). Thus, even among those samples selected at the local GFP maxima, voltage topography was more stable during moments when the electric field strength was high compared to when field strength was lower.

Global Field Power and Topographic Stability as Predictors of Microstate Fitting

The dependence of the microstate fitting procedure on the strength and topographic stability of the electric field was next examined. Maximal spatial correlations were calculated between EEG samples and each of the five global microstate cluster centroids. Figure 6 depicts 3D scatterplots between GFP, DISS, and the maximal spatial correlation of samples with microstates. As can be seen, voltage maps of samples with high GFP had uniformly greater spatial correlations than those samples with lower GFP.

This was confirmed by strong positive correlations for individuals on average between log-transformed GFP and the Fisher r to z-transformed spatial correlation with microstate cluster centroids in the eyes closed (*mean* $r = 0.557$, $SD = 0.043$, 95% CI [0.551, 0.563]) and eyes open conditions (*mean* $r = 0.553$, $SD = 0.041$, 95% CI [0.548, 0.559]). Log-transformed DISS only explained a small amount of additional variance in the z-transformed spatial correlations over and above log-transformed GFP in the eyes closed (*mean* $\Delta R^2 = 0.027$, $SD = 0.016$, 95% CI [0.025, 0.029]) and eyes open conditions (*mean* $\Delta R^2 = 0.020$, $SD = 0.015$, 95% CI [0.018, 0.022]). Samples selected at the local GFP maxima, however, had only a minimally larger spatial correlation with one of the five global microstate configurations than all remaining samples in the eyes closed ($M_{diff} = 0.029$, $SD = 0.008$, 95% CI [0.028, 0.030]) and eyes open conditions ($M_{diff} = 0.024$, $SD = 0.008$, 95% CI [0.023, 0.025]). These findings suggest that moments of high electric field strength were not only more topographically stable than when field strength was low but also better resemble the voltage topography of the five global microstate configurations.

Discussion

The basic premise underlying segmentation of broadband EEG into microstates based on momentary periods of topographic stability is well supported by empirical data in the present study. 191 healthy adults demonstrated strong and consistent associations between the GFP of samples and the topographic dissimilarity of temporally adjacent voltage maps. Voltage maps of samples selected at the local GFP maxima were also systematically less dissimilar from temporally adjacent samples compared to other samples in the EEG. These findings support the notion that the time series succession of voltage maps exhibit momentary topographic stability when the electric field strength is high. When the field strength was low, however, topographic stability varied considerably. That is, points of low field strength ranged across the entire distribution of values of topographic dissimilarity. After all, samples selected at the local GFP maxima also frequently occurred at points of low GFP relative to the entire distribution, though they were consistently more topographically stable relative to other samples. Selecting time series samples at the local GFP maxima therefore appears to be a good heuristic for identifying optimal points of topographic stability for clustering and microstate labeling.

The reported findings were also highly consistent across individuals. The strong association between log-transformed GFP and topographic stability was observed across thousands of samples of the EEG time series in every recording included in the present study. Yet, there was also some variability in terms of the magnitude of these correlations, and only 34% of the variance was shared between eyes closed

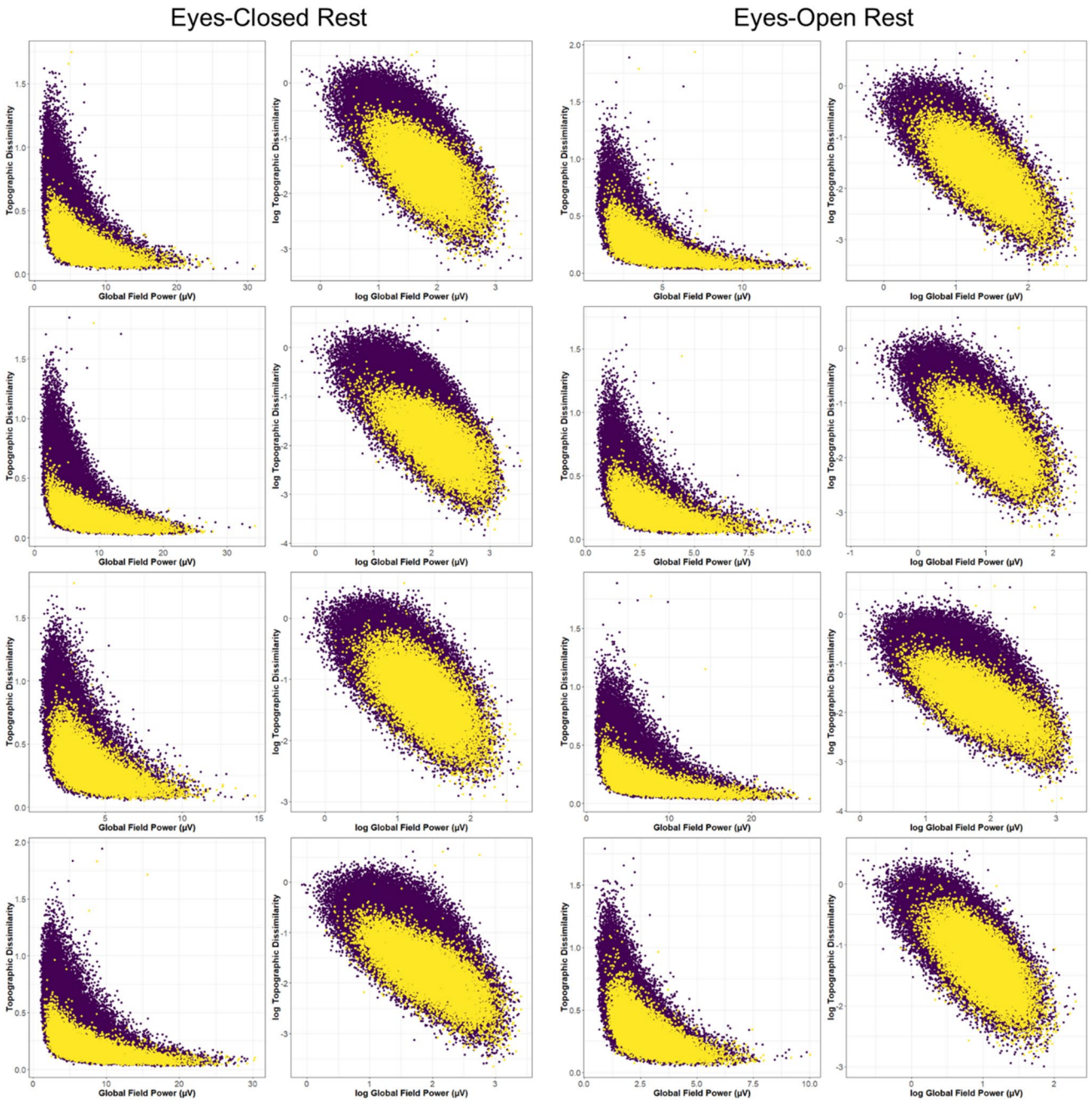

Fig. 5 Scatterplots depicting the global field power (GFP) and topographic dissimilarity between temporally adjacent (*sample t* and *sample t* – 1) voltage maps for samples (in yellow) selected at the local GFP maxima in the EEG time series. The remaining samples are in purple. The same EEG recordings are shown from Fig. 3

and eyes open conditions. This suggests that associations between GFP and topographic stability appear to quantify aspects of spatiotemporal dynamics that vary within individuals, which likely depend on the prevalence of noise and artifact in the EEG recording and variation in perceptual and cognitive states that condition the magnitude of synchronized oscillations over subsequent moments.

Clustering of EEG voltage maps at GFP peaks led to the identification of five data-driven microstate configurations that explained more than 60% of the total topographic variance when fit to individuals' EEG time series (Zanesco et al. 2020). The spatial correlation between voltage maps at samples of the EEG time series and these five microstate configurations were found to strongly correlate with the strength

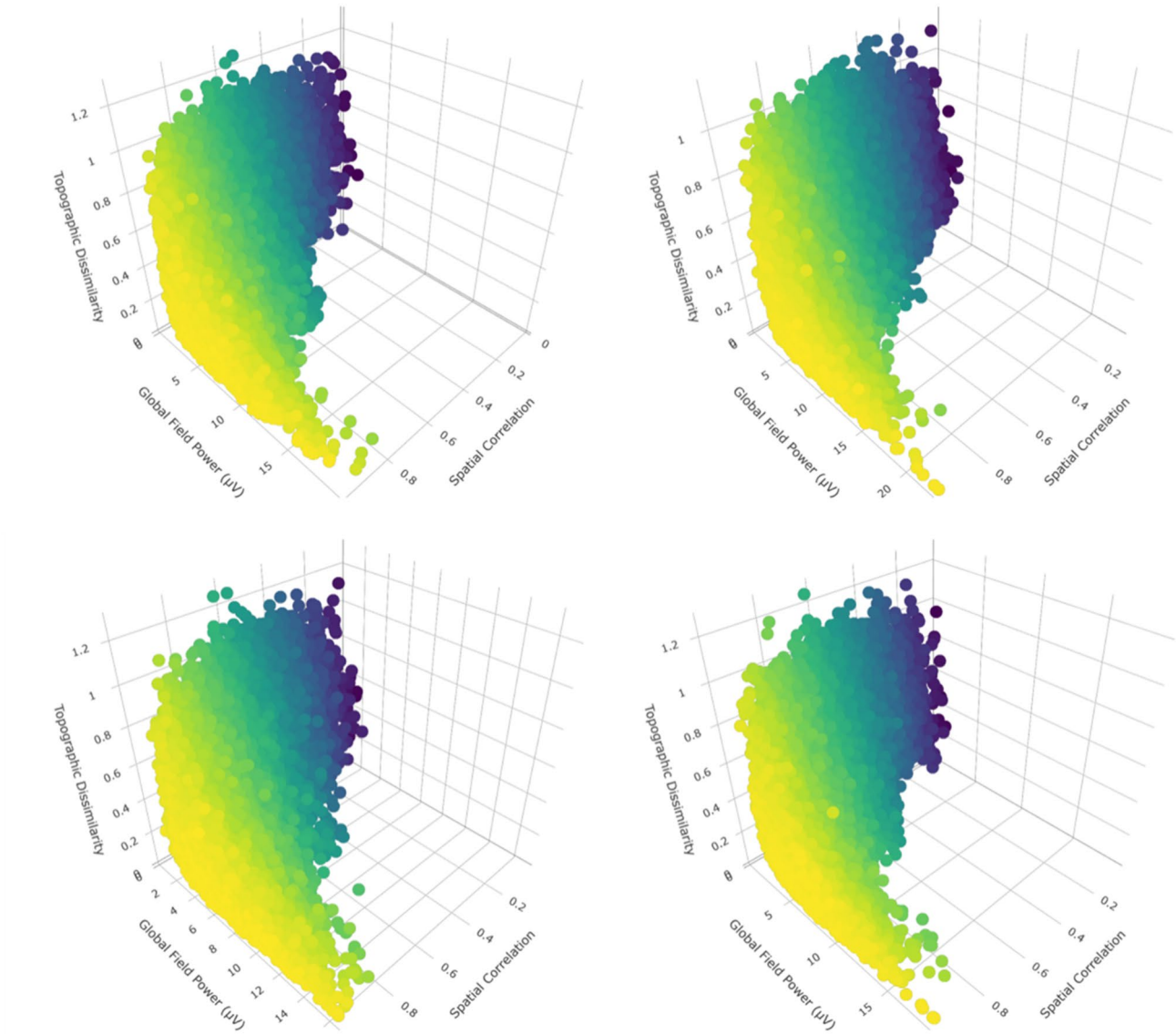

Fig. 6 3D scatterplots depicting samples of global field power (GFP) by topographic dissimilarity between temporally adjacent (*sample t* and *sample t -1*) voltage maps and the maximal spatial correlation between samples and the five microstate cluster centroids. Four eyes closed EEG recordings are shown selected at random. The spatial correlations of samples are indicated based on their color (from low spatial correlation in purple to high correlation in yellow)

and topographic stability of the electric field. This association was largely driven by variation in GFP magnitude, as the topographic dissimilarity of adjacent samples only explained a small amount of additional variance in the spatial correlation between microstates and voltage maps above that explained by GFP. Moments of strength in the electric field were not only more topographically stable than when field strength was low but also better resembled the voltage topography of the global microstate configurations. This is perhaps expected as microstate clusters are themselves derived from voltage maps at local GFP maxima, and were consistently more topographically stable relative to other samples.

Microstate clustering is commonly applied to voltage maps generated at the GFP peaks of the EEG time series because of the well-reasoned assumption that these instances maximize signal-to-noise ratio and provide optimal representations of the momentary quasi-stable voltage topography. Furthermore, moments of high GFP correspond to instances of greatest momentary synchronization in the activity of brain generators. While the present findings provide additional empirical support for the notion that clustering at local GFP maxima produces microstate configurations that optimally represent moments of topographic stability, this does not imply that clustering at other moments of the EEG time series

will not produce representative cluster solutions. In fact, there was considerable variability in the similarity of adjacent voltage maps at moments when GFP was lower. Common topographic patterns may therefore still be identified based on clustering applied to other moments of the EEG time series.

In line with other studies examining the limitations of common methods for segmenting EEG into microstates (Dinov and Leech 2017; Mishra et al. 2020), the present findings demonstrate some of the variability and uncertainty in microstate labeling and clustering. Indeed, many samples in the EEG, including those selected at the local GFP maxima, had a low spatial correlation with one the five microstate configurations identified in the present study. Clustering of topographic patterns into microstate configurations is fundamentally a process of data reduction that seeks to identify the optimal number of topographic patterns present in the EEG that are shared within or between individuals. These clusters of voltage maps may be more continuous than assumed by a discrete model of microstates (Mishra et al. 2020), leading to uncertain categorization of EEG samples. Alternatively, clustering solutions commonly limit the number of microstates to four configurations, which may fail to adequately capture the range of discrete microstate clusters present in the EEG (Michel and Koenig 2018). Finally, the microstate model assumes that residual variance in the fit of microstates primarily results from noise. It will be important for studies to attempt to quantify how much noise might contribute to variability in the fit of microstates, perhaps by simulating the contribution of transiently oscillating sources in the presence of differing levels of noise. Future studies should continue to evaluate these and other assumptions of the microstate model, as well as developing more probabilistic approaches for microstate categorization that can better account for uncertainty in assignment (cf. Dinov and Leech 2017).

In total, the present findings provide strong empirical support for the proposal that periods of topographic stability can be identified in the time series succession of voltage maps corresponding to common microstate configurations, and that moments of high field strength are optimal representations of quasi-stable electric field topography. The activity of phase-synchronized neuronal networks thus persists in a coherent topographic configuration for brief moments before quickly transitioning to different configurations. This agrees with the premise underlying microstate segmentation that ongoing brain activity can be parsed into sequences of coordinated brain states (Lehmann et al. 1987). Topographic stability during moments of high field strength therefore appears to be a basic property of the spontaneous spatiotemporal dynamics of the neuroelectric field.

References

Babayan A, Erbey M, Kumral D, Reinelt JD, Reiter AMF, Röbbig J, Villringer A (2019) A mind-brain-body dataset of MRI, EEG, cognition, emotion, and peripheral physiology in young and old adults. Sci Data 6:180308

Brechet L, Brunet D, Birot G, Gruetter R, Michel CM, Jorge J (2019) Capturing the spatiotemporal dynamics of self-generated, task-initiated thoughts with EEG and fMRI. Neuroimage 194:82–92

Britz J, Van De Ville D, Michel CM (2010) BOLD correlates of EEG topography reveal rapid resting-state network dynamics. Neuroimage 52:1162–1170

Brunet D, Murray MM, Michel CM (2011) Spatiotemporal analysis of multichannel EEG: CARTOOL. Comput Intell Neurosci 2(1–2):15

Custo A, Van De Ville D, Wells WM, Tomescu MI, Brunet D, Michel CM (2017) Electroencephalographic resting-state networks: source localization of microstates. Brain Connect 7(10):671–682

Dinov M, Leech R (2017) Modeling uncertainties in EEG microstates: analysis of real and imagined motor movements using probabilistic clustering-driven training of probabilistic neural networks. Front Hum Neurosci 11:534. https://doi.org/10.3389/fnhum.2017.00534

Khanna A, Pascual-Leone A, Michel CM, Farzan F (2015) Microstates in resting-state EEG: current status and future directions. Neurosci Biobehav Rev 49:105–113

Koenig T, Brandeis D (2016) Inappropriate assumptions about EEG state changes and their impact on the quantification of EEG state dynamics. Neuroimage 125:1104–1106

Lehmann D, Ozaki H, Pal I (1987) EEG alpha map series: brain microstates by space-oriented adaptive segmentation. Electroencephalogr Clin Neurophysiol 67:271–288

Michel CM, Koenig T (2018) EEG microstates as a tool for studying the temporal dynamics of whole-brain neuronal networks: a review. Neuroimage 180:577–593

Michel CM, Koenig T, Brandeis D (2009) Electric neuroimaging in the time domain. In: Michel CM et al (eds) Electrical neuroimaging. Cambridge University Press, Cambridge, pp 111–144

Mishra A, Englitz B, Cohen MX (2020) EEG microstates as a continuous phenomenon. NeuroImage 208:116454. https://doi.org/10.1016/j.neuroimage.2019.116454

Murray MM, Brunet D, Michel CM (2008) Topographic ERP analyses: a step-by-step tutorial review. Brain Topogr 4:249–264

Seitzman BA, Abell M, Bartley SC, Erickson MA, Bolbecker AR, Hetrick WP (2017) Cognitive manipulation of brain electric microstates. Neuroimage 146:533–543

Skrandies W (1990) Global field power and topographic similarity. Brain Topogr 3(1):137–141

Vaughan HG (1982) The neural origins of human event-related potentials. Ann N Y Acad Sci 388(1):125–138

Wackermann J, Lehmann D, Michel CM, Strik WK (1993) Adaptive segmentation of spontaneous EEG map series into spatially defined microstates. Int J Psychophysiol 14:269–283

Wittchen H-U, Zaudig M, Fydrich T (1997) SKID. Strukturiertes klinisches interview für DSM-IV. Achse I und II. Handanweisung. Hogrefe, Göttingen

Zanesco AP, King BG, Skwara AC, Saron CD (2020) Within and between-person correlates of the temporal dynamics of resting EEG microstates. NeuroImage 211:116631. https://doi.org/10.1016/j.neuroimage.2020.116631